Effect of the Heat Source Distribution in the Earth's Core on the Stability of Geodynamo

Project Representative
Yozo Hamano Institute for Research on Earth Evolution, Japan Agency for Marine-Earth Science and Technology

Authors
Yusuke Oishi Department of Earth and Planetary Science, University of Tokyo
Ataru Sakuraba Department of Earth and Planetary Science, University of Tokyo
Yozo Hamano Institute for Research on Earth Evolution, Japan Agency for Marine-Earth Science and Technology

We investigate the effect of the heat source distribution on the behavior of the magnetohydrodynamic (MHD) dynamo action. We consider three models in which the ratio of the heat flow at the inner core boundary to that extracted away from the core to the mantle varies from 0%, 50% to 100%. The most frequently studied geodynamo model with a temperature difference between the upper and lower boundaries corresponds to the 100% case. An important parameter closely related with the thermal condition is the Rayleigh number, which is defined as it indicates the amount of heat flow taken away from the core surface, and therefore, we performed a parameter study by changing the Rayleigh number as another control parameter. The results suggest that both the Rayleigh number and the heat source distribution influence the stability of the magnetic field. We also performed the case without the inner core to investigate the geometrical effect of the inner core on the dynamo action. The representative results of the simulations are summarized in this report.

Keywords: Geomagnetic-field, inner-core, geodynamo, magnetohydrodynamics

1. Introduction

In previously studied numerical geodynamo models, several aspects of the Earth's magnetic field have been reproduced, such as the dipole-dominant field and the time-variation characteristics, including polarity reversal. However, the numerical dynamos do not model the actual physical condition of the Earth's core at least in some respects, and therefore it is unclear to what extent the numerical results approximate the Earth's dynamo. One of the crucial differences between the models and the real Earth can be found in kinematic parameters. In particular, treating extraordinarily low viscosity of the Earth's core requires too high-resolution simulations to be implemented by using present-day computer systems. Based on this viewpoint, attempts have been made to achieve a parameter regime that is close to that of the Earth's core by using the highest possible computing power (e.g., Takahashi et al., 2005).

The thermal condition is also an important issue in comparing the models and the Earth. In most of the previously studied models, convection is driven by a temperature difference between upper and lower boundaries. However, this condition does not properly reflect that of the Earth's core. The driving force of the convection in the Earth's core is not entirely understood, but the following causes are conceivable to create buoyancy forces (e.g., Buffet et al., 1996): (1) secular cooling due to heat transfer from the core to the mantle, (2) internal heating by radiogenic isotopes (e.g., ^{40}K), (3) latent heat due to the inner core solidification, and (4) compositional buoyancy due to the ejection of light elements at the inner core surface. The latter two coincide with the inner core growth, which is ultimately caused by the secular cooling of the core. The relative contribution of the driving forces is not well-known, and it has probably changed in geological time-scales. However, all of the above phenomena except for radiogenic heating are caused by the secular cooling of the core and, therefore, any dynamo models that do not consider this effect might be dissimilar to the Earth's dynamo.

The thermal condition of the core has a considerable influence on the core convection. For example, in the case of a temperature difference between the outer and inner boundaries, the heat flow per unit area at the inner boundary is approximately ten times larger than that at the outer boundary, thereby causing enormously intense flows localized at the inner boundary. Some numerical dynamo models suggest that the reversal of the magnetic field is triggered by the strong fluctuations of the flow localized at the inner boundary, without incorporating secular cooling of the core (e.g., Takahashi et al., 2005). Since the assumption of no secular cooling is unrealistic, it is uncertain whether or not the strong flows near the inner core surface produced by the artificial boundary condition is really the very reason of the geomagnetic field reversals.

Here, we investigate the effect of the thermal condition on the behavior of the magnetohydrodynamic (MHD) dynamo action with the viscosity as low as possible. In this study, we consider three models in which the ratio of the heat flow put into the core at the inner boundary to that extracted away from the core to the mantle varies from 0%, 50% to 100%. The frequently studied model with a temperature difference between the upper and lower boundaries corresponds to the 100% case. Furthermore, the case without the inner core is also studied to clarify the geometrical effect of the inner core, where the ratio of the heat flow is 0%. Note that the case without the inner core is applicable to the Earth's core in the era before the inner core formation, which is often estimated as in the Proterozoic or in the Archean (e.g., Stevenson en al., 1983). An important parameter closely related with the thermal condition is the Rayleigh number, *Ra*, and therefore, we performed a parameter study by changing *Ra* as another control parameter.

2. Model

We consider a spherical shell filled with an electrically conductive Boussinesq fluid and spun around the z-axis with an angular velocity Ω. The ratio between the inner radius r_i and the outer radius r_o is set to 0.35 in the case with the inner core. The case without the inner core is also considered. The regions inside and outside the fluid shell are electrically insulating. The temperature of the inner core surface, if exists, is horizontally homogeneous, but its value changes in time due to heat transport between the inner and the outer cores. The average temperature of the outer surface of the core does not change in time, but the temperature variation over the outer surface is determined so that the heat flux per unit area is horizontally homogeneous. Rigid boundary conditions are imposed and both boundaries are co-rotating. The gravity changes linearly with radius. Spherical polar coordinates (r, θ, ϕ) rotating with an angular velocity $\Omega \boldsymbol{e}_z$ are used, where $\boldsymbol{e}_z$ is the unit vector parallel to the z-axis. The cylindrical coordinates (s, z, ϕ) are also used for illustrative purposes.

The nondimensional governing equations are

$$Em\frac{\partial \mathbf{u}}{\partial t} = E\nabla^2\mathbf{u} + Em\mathbf{u}\times\omega - \nabla\left(p + \frac{1}{2}Em\mathbf{u}\cdot\mathbf{u}\right) + \mathbf{u}\times\mathbf{e}_z + \mathbf{J}\times\mathbf{B} + qRaT\frac{\mathbf{r}}{r_o},$$

$$\frac{\partial \mathbf{B}}{\partial t} = \nabla^2\mathbf{B} + \nabla\times(\mathbf{u}\times\mathbf{B}),$$

$$\frac{\partial T}{\partial t} = q\nabla^2 T - \mathbf{u}\cdot\left[\nabla T - \left((1-Q)\left(\frac{r}{r_o}\right) + Q\left(\frac{r_o}{r}\right)^2\right)\mathbf{e}_r\right],$$

$$\nabla\cdot\mathbf{u} = \nabla\cdot\mathbf{B} = 0,$$

where $\boldsymbol{u}$, $\boldsymbol{B}$, $\omega = \nabla\times\boldsymbol{u}$, and $\boldsymbol{J} = \nabla\times\boldsymbol{B}$ are velocity, magnetic field, vorticity, and electric current density, respectively. T and p are deviations from the equilibrium state of temperature and pressure. Length is scaled by r_o, time by r_o^2/η, magnetic field by $\sqrt{2\rho\mu_o\eta\Omega}$ and temperature deviation by βr_o, where μ_o the magnetic permeability, η magnetic diffusivity, ν kinematic viscosity and ρ density. The resulting five nondimensional parameters are the modified Rayleigh number *Ra*, the Ekman number *E*, the magnetic Ekman number *Em*, the Roberts number q, and the heat source parameter, Q, which are defined by

$$E = \frac{\nu}{2\Omega r_o^2},\ Ra = \frac{\alpha\beta g_o r_o^2}{2\Omega\kappa},\ Em = \frac{\eta}{2\Omega r_o^2},\ q = \frac{\kappa}{\eta},\ Q = \frac{Q_1}{Q_0},$$

where α and g_o are the thermal expansion coefficient and acceleration due to gravity at the outer radius, respectively. Q_1 represents the heat flow added at the inner core surface and Q_0 does the total heat flow taken away from the core to the mantle. Note that the same Rayleigh number means the same heat flow across the core-mantle boundary, since the temperature is scaled by βr_o. When convection occurs to cool the core and transport the heat to the mantle, the heat flow across the core surface transiently increases. However, after the convection becomes a steady (or quasi-steady) state, the heat flow returns to the initial value because heating due to magnetic and viscous diffusions is neglected. In all the simulation in this study, the Ekman and magnetic Ekman numbers are set to 10^{-5}, and the Roberts number is set to 1. The Rayleigh number, *Ra*, and the heat source parameter, Q, are changed. The simulation code used here is based on the spectral transform method in which the variables are expanded by spherical harmonics and the Chebyshev polynomials. The initial condition of this study is the result of the magnetoconvection calculation with the same parameters or the result of the calculation with different but the nearest parameter. The spatial resolution is determined so that the wavenumber power spectra of all variables drop more than three orders of magnitude at the cutoff wavenumber, compared to the peak values of the spectra. The cutoff wavenumber used in this study is between 128 and 256.

3. Results

We examined the following four dynamo models:

1. Case N: the inner core does not exist, and heating is 100% internal (Q = 0.0),
2. Case E0: the inner core exists, and heating is 100% internal (Q = 0.0),
3. Case E1: the inner core exists, and heating is 50% internal and 50% from below (Q = 0.5), and
4. Case E2: the inner core exists, and heating is 100% from below (Q = 1.0).

Comparing Case N with Case E0 reveals the geometrical effect of the inner core. A comparison between Cases E0, E1, and E2 reveals the effect of a difference of the heat source distributions. Case E2 is practical comparing this study to other geodynamo models driven by only basal heating, which are common in most of the recent studies (e.g., Christensen and Aubert, 2006; Takahashi et al., 2005). Another control parameter We take notice in this study is the Rayleigh number *Ra*, which is changed from 200 to 19200. (The critical values of *Ra* for the convection are 200, therefore the calculation in this study reaches nearly 100 times critical.) We found 27 self-sustained dynamos out of 31 simulations with different conditions.

3.1 Three kinds of dynamo regimes

In the previous studies focused on the *Ra* dependency of the geodynamo (Takahashi and Matsushima, 2005; Kutzner and Christensen, 2002), the following three regimes have been observed on the basis of the value of *Ra*:

- low-*Ra* regime: the magnetic field is dipolar, and the magnetic energy increases efficiently with the increase of *Ra*,
- moderate-*Ra* regime: the magnetic field is dipolar, and the magnetic energy does not increase efficiently with *Ra*, and
- high-*Ra* regime: the magnetic energy decreases from that in the moderate-*Ra* regime; further, the magnetic field becomes non-dipolar, in contrast to the dipole-dominant magnetic field in the low- and moderate-*Ra* regimes.

The kinetic energy increases nearly linearly with the increase of *Ra*. In the present study, we identified the low- and the moderate-*Ra* regimes, which is universal irrespective of the variation of *Q* and the existence of the inner core. Although its calculation time is relatively short, the high-*Ra* regime was also found. These three kinds of regimes can be confirmed in Fig. 1. The spatial structure in each regime is shown in Fig. 2. Simulation lengths in all cases in the low-

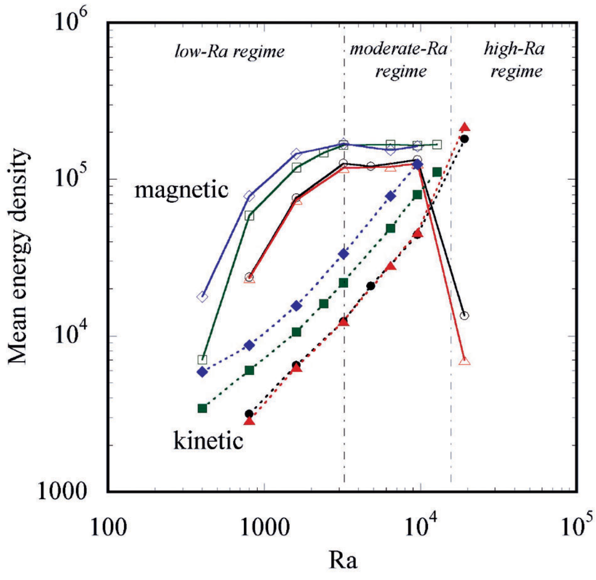

Fig. 1 Mean kinetic (filled symbols) and magnetic (open symbols) energy densities are plotted versus *Ra*. Case N (black), Case E0 (red), Case E1 (green) and Case E2 (blue).

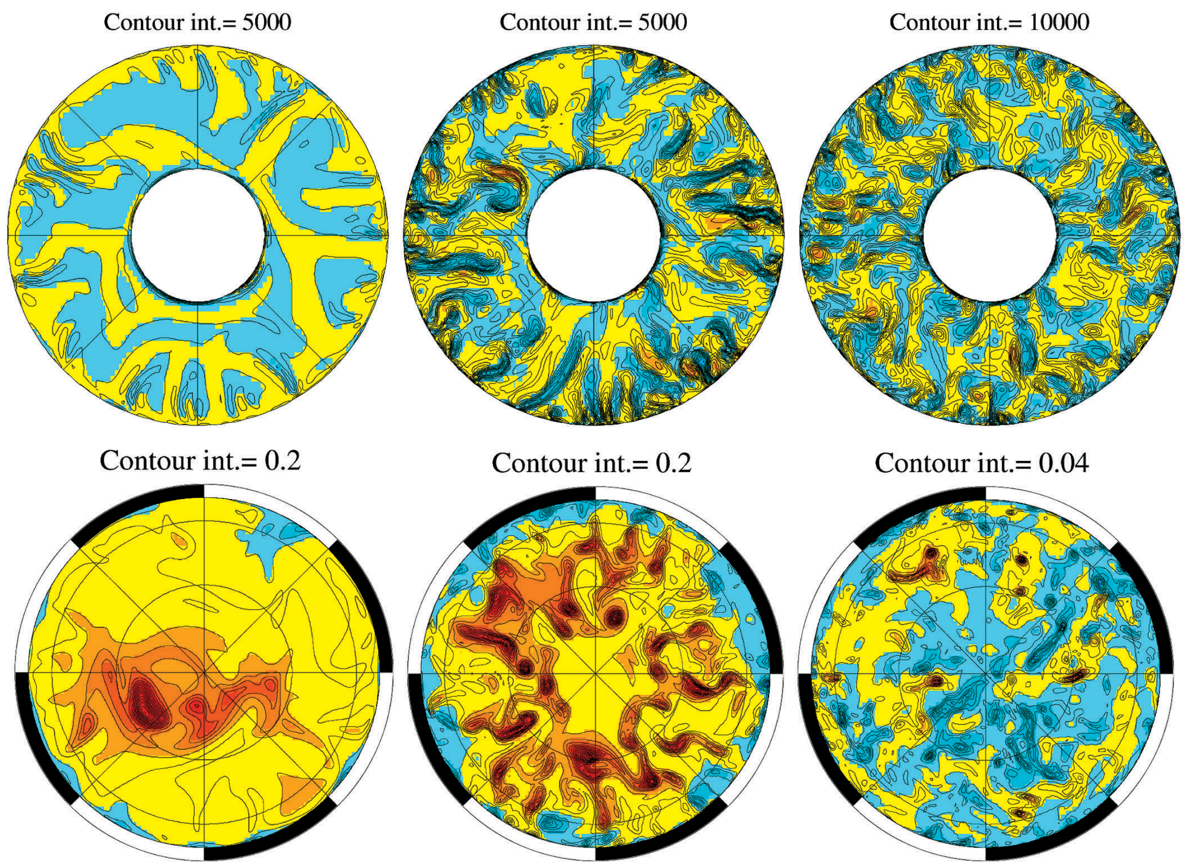

Fig. 2 Case E0. View from the North Pole. Warm colors indicate positive values and cold colors do negative values. (top) Axial vorticity ω_z in equatorial plane. (bottom) Radial magnetic field B_r at the outer shell surface. From left to right, *Ra* = 1600, 9600, and 19200.

and the moderate- regimes are at least longer than 0.6 time units, which is about 2.5 dipole diffusion times (one dipole diffusion time is about 0.24 time units). The simulation lengths in the high-*Ra* regime are shorter than 2.5 dipole times at this time, therefore we will mainly discuss the first two regimes in this report.

The ratio of the magnetic to kinetic energy densities can be interpreted as "dynamo efficiency" because this quantity roughly measures how strong the magnetic field is generated for a given convection strength. To investigate how the change of the dynamo regime influences the dynamo efficiency, the spectral distribution of the kinetic and the magnetic energy densities and the dynamo efficiency, *Em*/*Ek*, as a function of the harmonic degree *l* is shown in Fig. 3 and Fig. 4, respectively. In the low-*Ra* regime, the increase in the value of *Ra* causes no significant changes in the efficiency

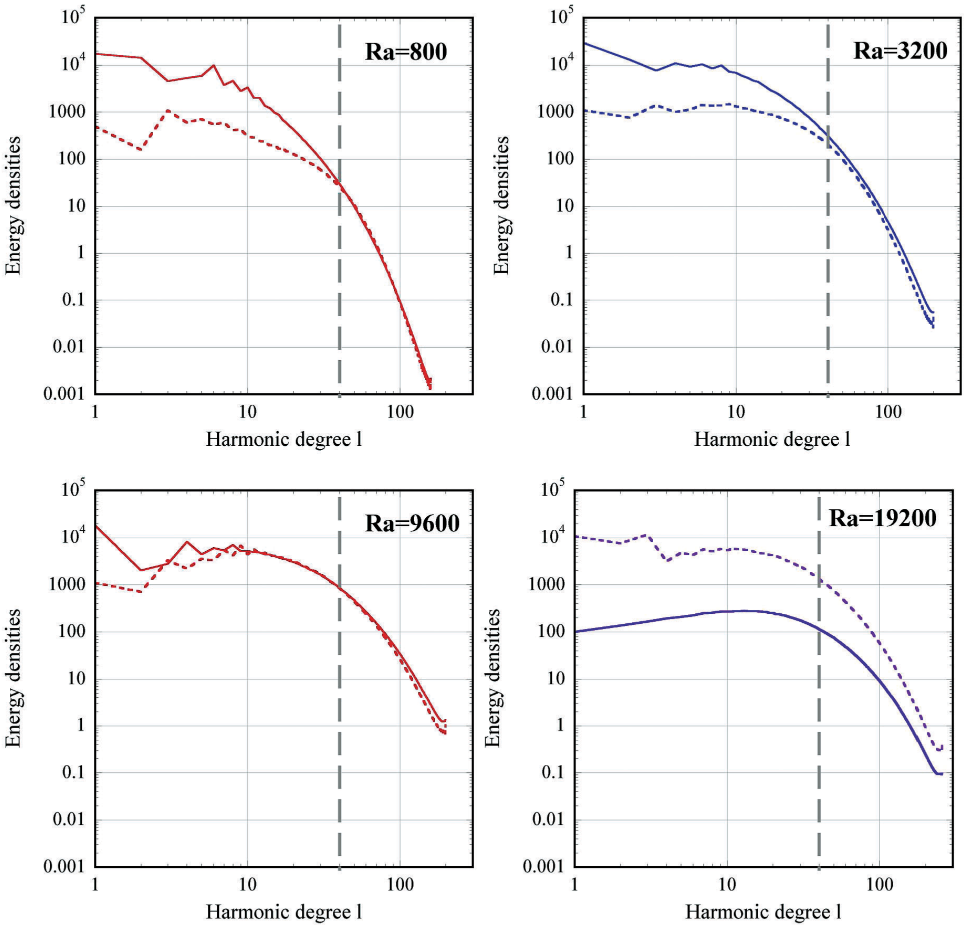

Fig. 3 Time-averaged spectra of the volume-averaged kinetic and magnetic energy densities. The solid lines indicate the magnetic energy densities and the dashed lines do the kinetic ones. Gray dashed lines indicate $l = 40$ as a marker. The results at $Ra = 800, 3200, 9600$ of Case E2 and result at $Ra = 19200$ of Case E0 are shown.

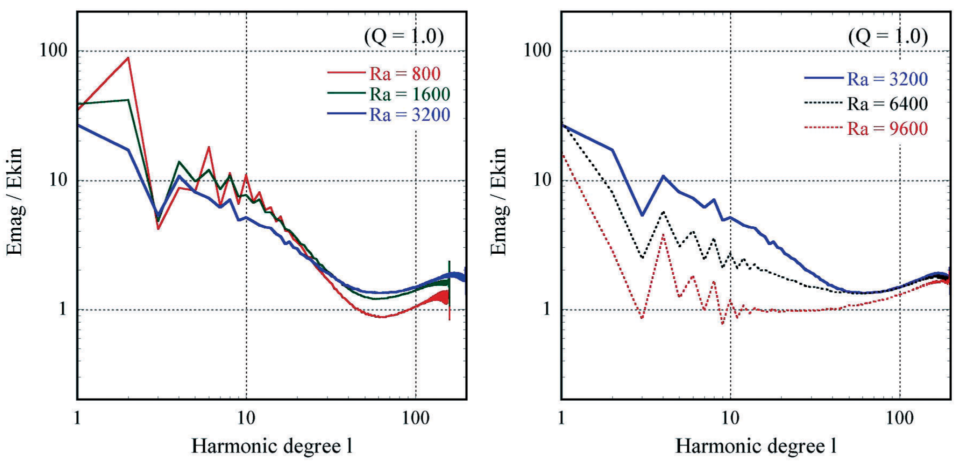

Fig. 4 The ratio of the magnetic energy spectral component to the kinetic one is shown for Case E2.

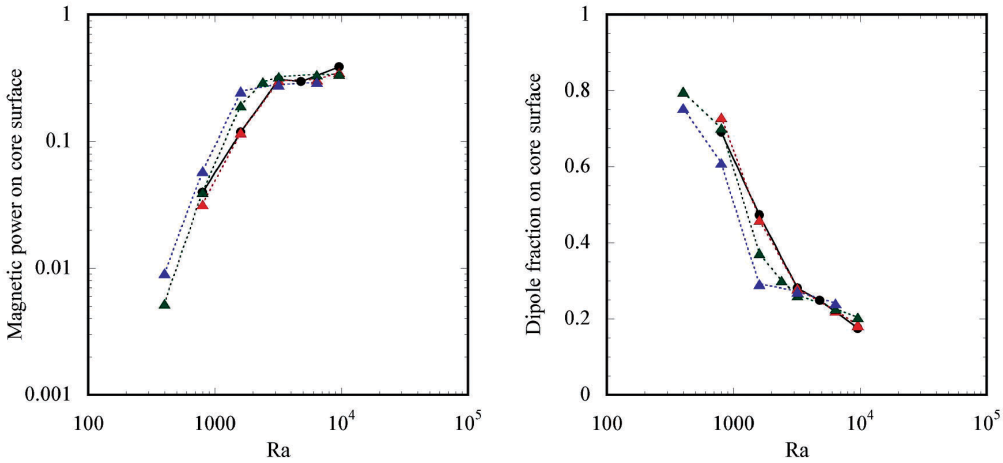

Fig. 5 Magnetic power at the core surface is plotted versus *Ra* (left) and Energy ratio of the dipole component to the total magnetic field on the core surface is plotted versus *Ra* (right). Case N (black), Case E0 (red), Case E1 (green) and Case E2 (blue).

spectrum (Fig. 4 (left)). On the other hand, in the moderate-*Ra* regime ($Ra \leq 3200$), the efficiency decreases with *Ra* especially in the high-*l* components, and the values of *Em*/*Ek* at these components approach unity (Fig. 4 (right)). This indicates that the increase in the small-scale components of the velocity fields in the moderate-*Ra* regime does not exhibit an efficient dynamo action.

3.2 Field intensity at the core surface

The spatial pattern and the intensity of the surface magnetic field are not affected very much by the addition of the basal heating and by the existence of the inner core, although the small-scale flux patches are expelled from the polar region in the cases with the inner core (see Fig. 7 (a)). Fig. 5 (left) shows the magnetic energy averaged over the core surface as a function of *Ra*. When the volume-averaged magnetic energy is saturated ($Ra > 3200$), the surface-averaged energy is also saturated in the same way. However, the saturated surface-averaged energies in all four cases are nearly the same, in contrast to the case of the volume-averaged magnetic energy where the addition of the basal heating creates 30% higher value (Fig. 1). This implies that the surface magnetic field intensity, which can be observed from the surface of the Earth, is independent of the addition of the heat sources at the inner core boundary, and that the difference of the volume-averaged magnetic energy due to the basal heating is caused by physical processes deep inside the core. The dipole fraction at the surface field gradually decreases with the increase in *Ra* as shown in Fig. 5 (right).

3.3 Tilt of the dipole axis

The morphology of the magnetic field at the core surface influences the magnetic dipole tilt, which we define as the ratio of the equatorial dipole component to the axial dipole component. Fig. 6 shows the time-averaged dipole tilt as a

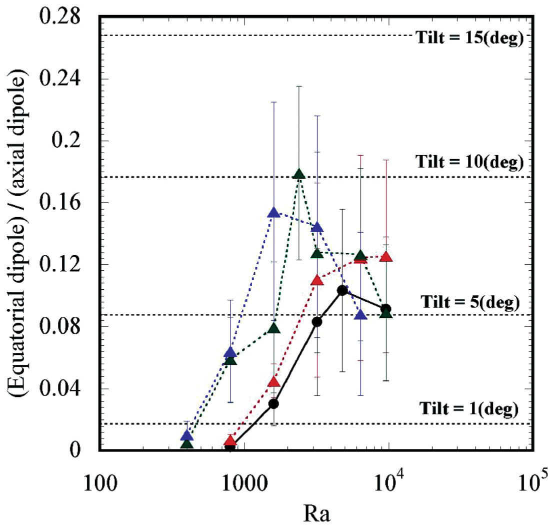

Fig. 6 The ratio of the equatorial dipole component to the axial dipole component is plotted versus *Ra*. The error bars denote the standard deviations. The corresponding dipole tilts are shown in the figures. Case N (black), Case E0 (red), Case E1 (green) and Case E2 (blue).

function of *Ra*. In all the cases, the averaged magnetic pole latitude regularly increases with *Ra* until $Ra = 3200$. However, at $Ra \geq 3200$, the magnetic pole latitude starts decreasing with *Ra*, particularly in Cases E1 and E2. The reason for this can be explained as follows. When one or a few number of magnetic flux patches comprise the dipole component (as in the result of $Ra = 1600$ in Fig. 2), the pole tilt is largely controlled by the motion of each patch. Since each patch basically tends to move with the flow beneath the core surface, whose fluctuation becomes more vigorous at higher *Ra*, the fluctuation amplitude of the patch becomes large and the dipole tilt increases at higher *Ra*. On the other hand, in the presence of several small-scale patches (as in the result of $Ra = 9600$ in Fig. 2), the pole tilt is determined as the average of the randomly distributed patches. In this case, the pole tilt becomes smaller when the small-scale patches are distributed more randomly as in the cases at higher *Ra*. As a result, the dipole tilt decreases with *Ra*.

3.4 Geometrical effects of the existence of the inner core

The absence of the inner core significantly influences the dynamics in the region near the rotating axis (the region s < 0.35). The axisymmetric flow along the rotating axis penetrating the equatorial plane appears when *Ra* is moderate, which creates a notable flux patch at the pole (Fig. 7 (a)). The magnetic patches' preference of the polar region in Case N results in a relatively smaller tilt than those in the other cases (Fig. 6). However, the difference of the convection pattern in the region s < 0.35 has negligible effect on the total dynamo efficiency because of small volume of this region. Therefore, the mean kinetic and magnetic energy densities in the case without the inner core are almost the same as in the case with the inner core and no basal heating (Fig. 1), indicating that there is no significant geometrical effect of the inner core on the dynamo efficiency.

3.5 Transition from the moderate- to the high-Ra Regimes

According to the previous studies (Takahashi and Matsushima, 2005; Kutzner and Christensen, 2002), the regime boundary between the dipolar moderate-*Ra* regime and the non-dipolar high-*Ra* regime corresponds to the state at which the kinetic and the magnetic energies are of the same order (i.e., *Em*~*Ek*). The same tendency was confirmed in our results as shown in Fig. 1. This indicates that the dynamo efficiency is closely related to the stability of the dipole field. The dynamo efficiency (*Em*/*Ek*) increases with *Ra* and reaches its maximum value at *Ra* = 1600 in all the four cases (Fig. 8 (left)). After that, the value starts decreasing linearly with *Ra*. The variation pattern of the dynamo efficiency reflects the change of the dynamo regime. The turning point at which the dynamo efficiency stops increas-

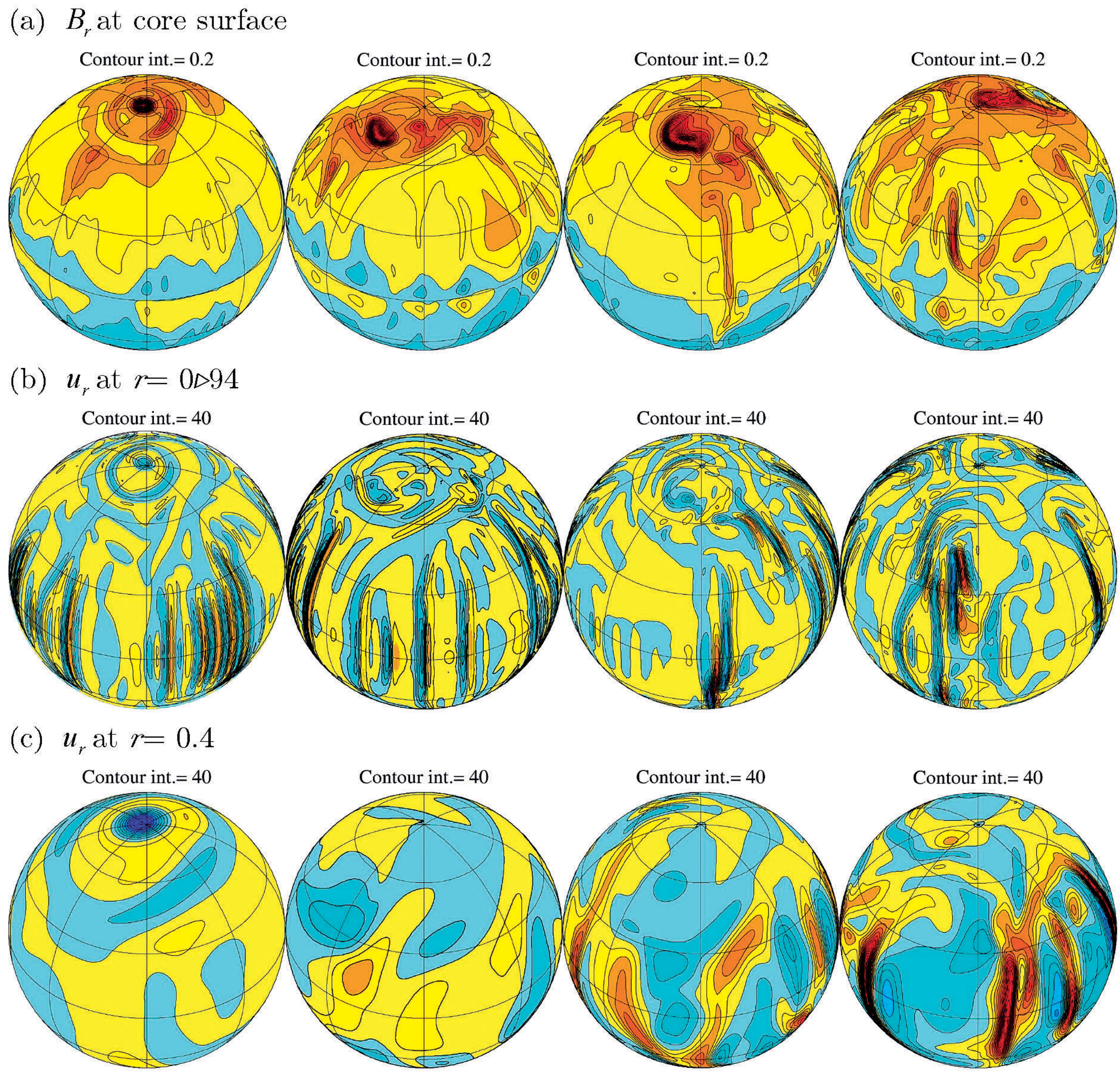

Fig. 7 The radial magnetic field B_r and velocity u_r at a certain depth. *Ra* = 1600. From left to right, Case N, Case E0, Case E1, and Case E2.

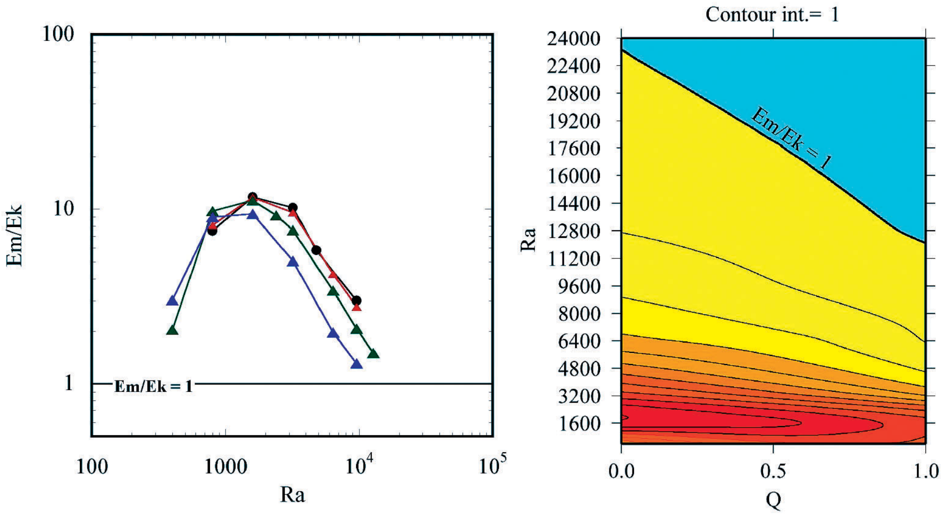

Fig. 8 Dynamo efficiency Em/Ek (ratio of the magnetic energy to the kinetic energy). In the left figure, Em/Ek is plotted versus *Ra* in Case N (black), Case E0 (red), Case E1 (green) and Case E2 (blue). In the right figure, Em/Ek is expressed as a contour map in the *Q*-*Ra* plane. The region where Em/Ek < 1 corresponds to the dynamo with unstable magnetic field.

ing probably corresponds to the transition from the low- to the moderate-*Ra* regimes. Here, we linearly extrapolate the value of *Em*/*Ek* in moderate-*Ra* regime to higher *Ra* to estimate a *Ra* value at which *Em*/*Ek*=1 in Fig. 8 (right). The difference in the values of the boundary *Ra* value in all the four cases implies that the destabilization tendency of the dipole field is greater in the cases with basal heating (Cases E1 and E2) than in the cases without it (Cases N and E0), and therefore, the change in the value of *Q* can cause the destabilization of the magnetic field.

4. Conclusion and Future works

We performed a parameter study of the MHD dynamo in the *Ra*-*Q* parameter space. As a result, it was found that the value of *Q*, which is the ratio between the heat flow added at the inner core surface and the total heat flow taken away from the core to the mantle, influences the stability of the geodynamo. In the previous studies, it was pointed out that the stability of the dynamo depends on the value of *Ra* (e.g., Kutzner and Christensen, 2002) and the morphology of the heat flow at the core mantle boundary (Glatzmaier et al., 1999). The result of this study can provide another possibility.

In the future work, the difference in the manner of the destabilization of dynamo between the cases with the different thermal condition should be closely studied to find out the effect of the thermal condition on the destabilization of the dynamo.

References

[1] B.A. Buffett, H.E. Huppert, J.R. Lister, and A.W. Woods, "On the thermal evolution of the Earth's core," J. Geophys. Res, vol.101, pp.7989–8006, 1996.

[2] U.R. Christensen, and J. Aubert, "Scaling properties of convection-driven dynamos in rotating spherical shells and application to planetary magnetic fields," Geophys. J. Int., vol.166, no.1, pp.97–114, 2006.

[3] G.A. Glatzmaier, R.S. Coe, L. Hongre, and P.H. Roberts, "The role of the Earth's mantle in controlling the frequency of geomagnetic reversals," Nature, vol.401, pp.885–890, 1999.

[4] C. Kutzner, and U.R. Christensen, "From stable dipolar towards reversing numerical dynamos," Phys. Earth Planet. Inter., vol.131, no.1, pp.29–45, 2002.

[5] D.J. Stevenson, T. Spohn, and G. Shubert, "Magnetism and thermal evolution of the terrestrial planets," Icarus, vol.54, pp.466–489, 1983.

[6] F. Takahashi, M. Matsushima, and Y. Honkura, "Simulations of a quasi-Taylor state geomagnetic field including polarity reversals on the Earth Simulator," Science, vol.309, pp.459–461, 2005.

[7] F. Takahashi, and M. Matsushima, "Dynamo action in a rotating spherical shell at high Rayleigh numbers," Phys. Fluids, vol.17, 076601, 2005.

地磁気ダイナモにおいてコア内の熱源分布が磁場の安定性に及ぼす影響

プロジェクト責任者
浜野　洋三　　独立行政法人海洋研究開発機構　地球内部変動研究センター
著者
大石　裕介　　東京大学大学院　理学系研究科　地球惑星科学専攻
櫻庭　　中　　東京大学大学院　理学系研究科　地球惑星科学専攻
浜野　洋三　　独立行政法人海洋研究開発機構　地球内部変動研究センター

地磁気ダイナモの再現を目的としたMHDダイナモシミュレーションの問題点として、流体核の粘性が極めて低いことにかかわるパラメータが、実際の地球において見積もられる値と大きく異っている点がしばしば指摘される。現在行われている多くの数値シミュレーションにおけるもう一つの問題点として、対流の駆動源が実際の地球の場合と異なっている点がある。地球の流体核における対流の駆動源としては、(1) 地球自体の冷却、(2) 放射性元素の崩壊に伴う発熱、(3) 内核の成長に伴う潜熱の放出、(4) 内核の成長に伴う軽元素の放出が考えられている (e.g., Buffett, 1996)。ただし、それらの相対的な寄与の割合はよく分かっていないのが現状である。一方で、シミュレーションモデルは上部・下部境界で温度を固定した下部加熱による熱対流モデルがほとんどである (e.g. Takahashi et al., 2005; Christensen & Aubert, 2006)。しかしながら、実際の地球は冷却しており、下部境界で浮力を生み出す (3)、(4) の駆動源もそもそもは地球の冷却に起因する。そのため、冷却を考慮しないダイナモモデルは現実的であるとはいえない。

そこで、本研究では冷却および下部からの加熱の双方を考慮し、下部加熱の寄与の割合が0%、50%、100%である3つのケースでのMHDダイナモシミュレーションを行い、熱源の分布がダイナモ作用に及ぼす影響を調べた。また、内核の無いケース（下部加熱の寄与は0%）のシミュレーションも行い、下部境界の有無の影響も調べた。エクマン数は10^{-5}、プラントル数・磁気プラントル数は1で固定し、レイリー数依存性を広範囲に渡って調べた。その結果、以下のような結果が得られた。(1) ダイポール磁場の卓越するlow-レイリー数領域、およびmoderate-レイリー数領域、非ダイポール磁場であるhigh-レイリー数領域が温度条件・内核の有無に依らず存在する。(2) コア表面の磁場は熱境界条件には依存せず、コアマントル境界の熱流量のみで決まる。(3) moderate-レイリー数領域においてダイポールの自転軸からの傾きは減少する。また、内核が無いケースでは内核があるケースよりもさらに傾きが小さい。(4) Kutzner & Christensen (2002)などにより磁場の安定性を支配することが指摘されているレイリー数のみならず、内核境界での熱源の分布の仕方も、また磁場の安定性に影響を与える可能性があることが示された。

キーワード：地磁気, 内核, ダイナモ作用, 電磁流体力学